HMG Advance Access published December 20, 2011

A single administration of morpholino antisense oligomer rescues spinal muscular atrophy in the mouse

Paul N. Porensky[1,2], Chalermchai Mitrpant[3], Vicki L. McGovern[1], Adam K Bevan[4]*, Kevin D Foust[4], Brain K Kaspar[4],Stephen D. Wilton[3], Arthur H.M. Burghes[1]

[1]Department of Molecular and Cellular Biochemistry, The Ohio State University, 363 Hamilton Hall, 1645 Neil Avenue, Columbus, OH 43210, USA.

[2]Department of Neurological Surgery, The Ohio State University Medical Center, N1014 Doan Hall, 410 W. 10th Ave, Columbus, OH 43210, USA.

[3]Centre for Neuromuscular and Neurological Disorders, University of Western Australia, Perth, WA 6009, Australia.

[4]Deparment of Gene Therapy, The Research Institute, Nationwide Children's Hospital, Columbus, Ohio, 43205

*Future address: Department of Neuroscience, The Ohio State University College of Medicine, Columbus, OH, 43210

Correspondence to: Burghes or Porensky; email burghes.1@osu.edu or paul.porensky@osumc.edu

Telephone 614-688-4759, Fax 614-292-4118

Abstract

Spinal Muscular Atrophy (SMA) is an autosomal recessive disorder characterized by α-motor neuron loss in the spinal cord anterior horn. SMA results from deletion or mutation of the *Survival Motor Neuron 1* gene (*SMN1*) and retention of *SMN2*. A single nucleotide difference between *SMN1* and *SMN2* results in exclusion of exon 7 from the majority of *SMN2* transcripts, leading to decreased SMN protein levels and development of SMA. A series of splice enhancers and silencers regulate incorporation of *SMN2* exon 7; these splice motifs can be blocked with antisense oligomers (ASOs) to alter *SMN2* transcript splicing. We have evaluated a morpholino oligomer against ISS-N1 (HSMN2Ex7D(-10,-29)), and delivered this morpholino (MO) to postnatal day 0 (P0) SMA pups (*Smn* -/-, *SMN2*+/+, SMNΔ7 +/+) by intracerebroventricular (ICV) injection. Survival was increased markedly from 15 days to over 100 days. Delayed CNS MO injection has moderate efficacy, and delayed peripheral injection has mild survival advantage, suggesting that early CNS ASO administration is essential for SMA therapy consideration. ICV treatment increased full-length SMN2 transcript as well as SMN protein in neural tissue, but only minimally in peripheral tissue. Interval analysis shows a decrease in alternative splice modification over time. We suggest that CNS increases of SMN will have a major impact on SMA, and an early increase of SMN level results in correction of motor phenotypes. Last, the early introduction by intrathecal delivery of morpholino oligomers is a potential treatment for SMA patients.

Introduction

Spinal Muscular Atrophy (SMA), the leading cause of hereditary infant mortality (1), is an autosomal recessive disorder characterized by α-motor neuron loss in the anterior horn of the spinal cord (2). SMA is caused by the loss or mutation of the *Survival Motor Neuron* (*SMN1*) gene and the retention of *SMN2* (3, 4). The *SMN1* and *SMN2* genes essentially differ at a single nucleotide in exon 7 (C to T transition) which disrupts a modulator of splicing and leads to exon 7 loss in 90% of *SMN2* mRNA transcripts (5-10). The SMN protein lacking exon 7 encoded amino acids does not oligomerize efficiently and is rapidly degraded, leading to low SMN levels and thus SMA (11-13). The *SMN2* copy number has a major influence on the severity of the SMA phenotype with milder patients (Type III-IV, juvenile/adult onset) having a higher *SMN2* copy number, Type II having intermediate *SMN2* copy number, and severe patients (Type I, infantile) having a lower *SMN2* copy number (14, 15). Furthermore, different *SMN2* alleles that are capable of producing more SMN act as improved modifiers of SMA (16, 17). Missense mutations occur in both mild and severe patients, (4, 18) such mutations in severe patients often disrupt the ability of SMN to oligomerize efficiently (12, 18). In the case of mild missense mutations, the SMN protein is often able to interact with wild type SMN produced by *SMN2*, resulting in more functional SMN complexes (19).

SMN forms a complex with a series of proteins called gemins, and the best characterized function of this complex is the assembly of Sm proteins onto snRNA, thus forming a crucial component of the splicing machinery (20-22). Thus, complete loss of *Smn* in mice is embryonic lethal, as SnRNPs are required for gene splicing (23). SMN has also been found in axons and is suggested to play a role in the axonal transport of mRNA (24-27). The exact role that SMN plays in the axon is unclear (4), and motor axon growth is not disrupted in SMA mice models (28). Reduced SnRNP assembly has been reported in SMA mice (29, 30), and certainly specific target genes could have disrupted splicing (4, 31). Yet controversy remains as to whether SMA is caused by the disrupted splicing of select genes important for motor neuron circuitry, or by disrupted axonal maintenance (4). It is well established that SMA is caused by insufficient SMN levels (32, 33) and thus current therapeutic strategies are focused on increasing the amount of SMN.

Mice possess only one *Smn* gene and the loss of this gene is embryonic lethal (23). Thus, the production of mice with an SMN deficiency that models human SMA required the introduction of the *SMN2* gene. Two copies of human *SMN2* in mice lacking *Smn* results in mice with severe SMA that live an average of 5 days, while 8 copies of *SMN2* results in complete rescue (34, 35). The introduction of SMNΔ7, an SMN transgene lacking exon 7, into the severe SMA mice increases the average life span to approximately 14 days (36). It has recently been shown that postnatal induction of SMN can modulate SMA in SMNΔ7 mice (37). The SMNΔ7 mice can therefore serve as an SMA model in which one can characterize disease modifying pharmacologic interventions.

Using the SMNΔ7 mouse model of SMA, multiple treatment strategies to increase SMN expression have been performed. Targeting SMN production with various pharmacologic compounds to either activate the SMN promoter (38, 39) (40), or to alter exon 7 splicing patterns (41), has shown modest improvements in the phenotype of SMNΔ7 SMA mice due to a relatively weak SMN induction. Restoration of SMN using scAAV9-SMN delivered via the facial vein in newborn SMNΔ7 SMA mice results in rescue of the phenotype with survival in all cases beyond 200 days (42, 43)and in one instance beyond 400 days(44). Thus, induction of SMN postnatally has a remarkable therapeutic effect.

Antisense oligomers (ASO), including 2'-O-methyl (2'-OMe) or 2'-O-Methoxyethyl (MOE) modified nucleotides on a phosphorothioate backbone, peptide nucleic acids (PNA), and phosphorodiamidate morpholino (MO) oligomers(45-47), can be used as specific splice switching agents to alter pre-mRNA processing. ASOs block or enhancing motifs involved in exon recognition and splicing, including exon splice enhancers (ESE) or intron splice silencers (ISS)(46-50). Numerous regions are important in *SMN2* splicing regulation (51), and one particularly important element is the negative splice regulator ISS-N1, a 15 nucleotide-splice silencing motif located downstream of *SMN2* exon 7 (52). An 18mer MOE chemistry ASO overlapping ISS-N1 effectively increases *in vivo* exon 7 incorporation and SMN levels through *SMN2* splice modulation (53, 54). Intracerebroventricular (ICV) injection of this MOE at a dose of 0.58mM did increase average survival in SMNΔ7 SMA mice from 14 days to 26 days (55). However, there was evidence of toxicity with this MOE at

doses greater than 1.16mM. More recently while this work was in review, Hua *et al* reported that peripheral dosing of MOEs was essential for longer survival, and propose that extra-CNS targets (i.e. peripheral) are required.for rescue of the SMA phenotype(56). This assertion contradicts previous results showing the necessity of neuronal SMN expression using both scAAV8-SMN delivery by ICV, and transgenic approaches which limit SMN expression to CNS or peripheral tissue (57, 58); moreover, the authors show CNS *SMN2* splicing modulation after serial high-dose peripheral deliveries, suggesting MOE transport across the blood-brain barrier when delivered at high doses in young mice.

Morpholinos have a low toxicity and a wide distribution of uptake as evidenced by their extensive use in target gene expression knockdown in the developing zebrafish (59). Morpholinos have been used to induce exon skipping in Duchenne muscular dystrophy (DMD) with excellent body-wide distribution and restoration of dystrophin expression after systemic administration in the *mdx* mouse (49, 60, 61). Likewise, there have been encouraging clinical results in patients with DMD after morpholino administration (62-64).

In this study, we delivered a bolus ICV injection of a high-concentration, highly-stable morpholino targeted to ISS-N1 to alter *SMN2* splicing and increase SMN levels. We have named this morpholino HSMN2Ex7D(-10,-29) (referred to as MO) based on its position relative to the exon 7 donor site. Treated SMA mice had improvement in weight gain, motor activity, and increased survival from 15 days to over 100 days. Peripheral facial vein (FV) delivery at P0, combined peripheral and ICV delivery, and dual ICV injection at P0 and P30 produced equivalent survival. Delayed CNS delivery (P4) had an intermediate advantage, evidence that earlier CNS treatment yields more robust effects, while delayed peripheral delivery after blood-brain-barrier maturation had only modest increased survival.

ICV injection yielded an increase in both *SMN2* exon 7 incorporation and SMN protein levels in brain and spinal cord, while digital droplet PCR (ddPCR) showed no alteration of *SMN2* splicing in peripheral tissues (kidney, liver, heart) with Smn+/- heterozygotes and small alterations with SMA animals. P0 FV delivery of MO clearly altered *SMN2* splicing within the CNS, evidence that the morpholino ASO does cross the blood-brain-barrier, but does not have effect across the CSF-blood barrier in young mouse pups. Immunofluorescence analysis of lumbar spinal cord sections delineates increased SMN and dissemination of the MO to caudal CNS

strucutures. These results suggest that it is essential to restore SMN levels within neurons to have a major impact in SMA, and long survival benefit can be obtained without significantly enhancing SMN levels in the periphery. It remains possible that increasing SMN expression in the ANS outside of the blood-brain-barrier may be required for full correction of SMA. These results support the continued investigation of morpholino ASOs in the early treatment of SMA.

Results

MO modulates exon splicing and increases SMN production

Mutation or steric block at the 5' region of *SMN2* intron 7 (ISS-N1) yields the greatest rates of exon 7 inclusion (51, 52, 54). We designed our morpholino (MO) to mask this splice silencing motif (Fig. 1). A sequence nonspecific scramble morpholino (referred to as scMO) was manufactured with identical length and molecular weight to MO. To assess exon 7 splicing inclusion, we injected by ICV newborn (P0) pups of genotype *Smn +/-; SMN2+/+; Δ7+/+* ('heterozygotes') with one of three doses of MO (high, middle, low dose) or scMO. Heterozygotes were used due to the normal phenotype (as a result of the presence of one *Smn* gene), thus controlling for additional splicing changes that could accompany an SMA mouse as well as secondary disease effects (*e.g.* poor nutrition, muscle atrophy). The availability of human specific primers and antibody facilitated analysis. Injected animals were sacrificed at interval ages with collection of brain, spinal cord, heart, liver, and kidney tissue. The total number of mice allowed analysis of all samples in triplicate. For assessment of exon 7 incorporation, we performed RT-PCR and then amplified the cDNA with *SMN2* specific primers. Amplification yields both a full-length (1491 nucleotides, top) and exon 7 deficient product (1433 nucleotides, bottom). scMO injected animals had a strong exon 7 deficient band, and transgenic animals with 16 copies of *SMN* (*8SMN2* +/+; *Smn* -/-; HiCopy or 'HiC') (35) also had a relative band intensity of exon 7 deficient greater than full-length. All MO injected heterozygotes showed a strong band reversal (full-length>exon 7 deficient) at all time points (P7→P65) in both brain (Fig. 2A) and spinal cord (Fig. 2B).

Quantification of full-length *SMN2* transcript was performed by both real time RT-PCR and ddPCR. The latter has many advantages for both quantification and detection of low levels of a specific transcript (65). The

sample is first partitioned into droplets, the distribution of any particular molecule (such as a specific cDNA) will conform to a poisson distribution. The number of droplets amplified by PCR is proportional to the concentration of that molecule. The end result is a count of positive droplets after the PCR has gone to completion. ddPCR has the ability to detect small amounts of a particular cDNA, and does not suffer from the logarithmic error seen in real time PCR. In our experience this method has been highly reliable in quantification when compared to real time PCR methods.

We performed ddPCR of P7 pup brain and spinal cord tissue injected at P0 with either MO (2, 4, or 6mM) or scMO (control). Figure 2C shows the full length *SMN2* response curve with escalating MO dose. We next quantified by real time RT-PCR full length *SMN2* transcript as a function of increasing animal age through P65 (Fig. 2D). Low, middle, and high P0 MO doses yielded an increase in exon 7 incorporation at P7, with a stable decay through day P65. It again should be realized that these increases in *SMN2* exon 7 incorporation are a result of a single P0 bolus dose, delineating the robust CNS stability of the morpholino.

We next asked whether CNS administered MO crosses the cerebrospinal (CSF)-blood barrier and remains sufficiently stable in the blood stream to affect systemic structures. These experiments aimed to characterize the importance of CNS vs. peripheral SMN expression. *SMN2* RNA splicing analysis was performed on CNS and systemic organs (heart, liver and kidney) one week after middle dose (4mM) MO injection into mice heterozygous for mouse Smn. The analysis was done by both RT-PCR and ddPCR RT-PCR of heart, liver, and kidney did not show subjective modulation of splicing in any visceral organ, though spinal cord again showed strong exon 7 incorporation (Fig. 3A). ddPCR (Fig. 3B) revealed no significant splicing changes in tissue outside the nervous system after ICV delivery (liver and heart). Furthermore, there was an increase in *SMN2* exon 7 incorporation within the CNS after peripheral delivery, suggesting that high doses of MO delivered peripherally do have the ability to cross the blood-brain-barrier in the physically immature neonatal mouse pup. We also injected SMNΔ7 SMA mice (n=2) by middle dose MO ICV and compared tissue *SMN*2 exon 7 incorporation to control SMNΔ7 SMA animals (Fig. 3C). As was seen with mSmn+/- heterozygotes, there were large CNS increases in full length *SMN*2, up to five-fold in both brain and

spinal cord. There were also smaller (2-fold) increases in liver, suggesting immaturity or derangement of the blood-CSF barrier in SMNΔ7 SMA mice, but again reinforcing the 'leakiness' of CSF barriers in neonatal pups. Taken together, these results are important for two reasons: first, the phenotypic changes seen in MO ICV injected SMA mice are most likely a result of the large amount of exon 7 splice modulation within the CNS relative to only modest splice modulation within the periphery, and second, peripherally administered MO in the neonatal mouse profoundly alters CNS *SMN2* splicing.

We quantified SMN protein levels after P0 ICV MO injection (Fig. 4). Primary antibody detected human SMN and did not have affinity for mouse SMN (53). At P7, all MO doses increased SMN levels (relative to β-actin) in both brain (Fig. 3A and 3C) and spinal cord tissue (Fig. 4B and 4D) as compared to scMO injected control animals. Again, as was seen with splicing changes, there was a decrease in relative SMN levels at later time points.

P0 MO was injected by ICV into SMNΔ*7* SMA mice which had motor neuron specific GFP expression (*Smn -/-; SMN2+/+;* Δ*7+/+;* HB9:GFP), and animals were sacrificed at P0 (66). Staining of lumbar cord sections with human SMN specific antibody showed gems in the nucleus and SMN staining in the cytosol of both motor neurons and spinal cord support cells (Fig. 5). There was robust evidence of SMN in the most distal segments of the spinal cord parenchyma. An ICV injected lissamine-tagged morpholino also showed lumbar cord parenchymal distribution (Fig. S1).

MO targeting ISS-N1 extends survival in SMA animals

SMNΔ7 SMA mice (*Smn -/-; SMN2+/+;* SMNΔ7+/+) were injected by P0 ICV with either MO at low (n=8), middle (n=10), or high dose (n=13), or with scMO (n=8). Control mice (*Smn +/+; SMN2+/+;* SMNΔ7+/+) were injected with scMO (n=30). Animals were weighed daily, assessed for morbidity (peripheral necrosis, acute weight loss, bladder or bowel retention, priapism, decreased grooming) and mortality, and righting response was tested through P21. MO injected animals had increased survival at all concentrations (Fig. 6A), with median survival increasing from 15±1.1 days (scMO) to 83± 37.7 days (MO, low dose), 104±15.0 days

(middle dose) and 112± 6.6 days (high dose). The survival advantage was significant for all three groups (Log Rank $p<0.001$), and was not significant between MO doses (Log Rank $p>0.8$); indeed, the low-dose strategy yielded our longest-lived mouse (161 days).

We also injected SMNΔ7 SMA mice with 5 µg (0.74mM, n=4) and 10 µg (1.48mM, n=3) MO (Fig. 6C); the former dose more closely approximates the MOE-ASO dose (0.58mM) that was reported to have some survival advantage (median 26 day survival) for the SMNΔ7 SMA model in a previous ICV ASO administration study by Passini *et al.* (55) . Though it is too early in these low-dose investigations to calculate median survival, through P26 there is a 75% survival with 5 µg injection, and 100% survival with 10 µg. Additionally, three mice were injected by ICV at P0, P1, and P2 with 135 µg MO (2 µl of 10mM MO) per dose for a total dose of 405 µg ICV. These mice, currently 38 days old, are healthy and show no evidence of toxicity. These results clearly indicate that long survival can be obtained with CNS delivery alone. Mortality was not increased as a result of CNS cannulation or MO injection. We did have 7 deaths among the 30 scramble control injected mice, though four mice were sacrificed iatrogenically due to injuries from fighting, cage flooding, and a grossly infected foot. No control mice died within the first week of life. Therefore, 3 of 30 control animals died from unknown causes, though none displayed declining weight before death. While it is plausible that control treatment contributed to this mortality, the lack of a pattern of animal decline and death in this group largely reinforces the safety of ICV cannulation and of the morpholino chemistry ASO.

Treated animals had weight gain nearly parallel to control animals through ~P30 (Fig. 6B) at which time the mass of treated animals stabilized at ~80% that of control animals (P80 average weight of SMA treated animals: low=16g, middle=17g and high=19g, vs. controls=22 g). There was normalization of righting response within days of treatment (Fig. 7A). Forelimb and hindlimb grip-strength at P30 showed equivalent force generation (per animal mass) in treated SMNΔ7 SMA mice as compared to controls (Fig. 7B).

MO treated mice developed an interesting phenotype of peripheral necrosis, similar to that seen in a previous study of early SMN modulation (34, 38, 44). All SMA mice had shorter tails during neonatal, adolescent, and early adulthood (Fig. S2A). Beginning at ~P50, both pinna and tails of SMA mice necrosed

until healing granulation tissue appeared at the base of these structures (Fig. S2B**)**. Three treated mice (one middle dose and two high dose) developed signs of possible autonomic nervous system dysfunction, including priapism, urinary retention and bowel obstruction. One middle dose and three high dose adult SMA animals died unexpectedly without evident morbidity (weight loss, decreased grooming, decreased activity, or urinary retention). These four mice weighed the most among all treated mice. This mortality suggests hyperacute cardiopulmonary failure as has been previously demonstrated in rescued mice of the SMNΔ7 SMA mouse model (67).

A variety of P0 injection modalities was attempted in an effort to investigate whether either a supplementary CNS dosing or targeting of peripheral structures (i.e. extra CNS autonomic nervous system) could increase animal survival and decrease necrosis. SMA mice were injected with a high dose MO through the peripheral facial vein (FV), as well as a combination of ICV and FV (Fig. 8). Additionally, another group received P0 ICV MO coupled with P30 stereotactic ICV injection (n=4). All of these administration techniques produced impressive survival advantage equivalent to but not greater than high dose PO ICV MO (Log Rank $p>0.09$ for all pairwise comparisons). Necrosis was not prevented or delayed in these groups. Mice treated with a single peripheral injection (50 µg/g animal mass, n=3) had a median survival of 35+/-6.5 days, with a maximum survival of 112 days, suggesting either peripheral MO toxicity or inadequate full-length SMN translation. Mice injected at P0 with both peripheral (50 µg/g) and ICV (54 µg, middle dose) MO, however, had substantial increases in median survival (93+/-6.4 days, n=5). These results evidence the non-toxicity of peripheral MO at this dose, as well as reinforce the central importance of CNS *SMN2* splice modulation.

A cohort of SMA animals was injected at P4 by ICV (n=5) to determine the extent of phenotype modification with delayed delivery. We chose delivery at P4 as this time-point approaches the latest age at which free-hand delivery can easily and reliably cannulate the lateral ventricle due to increasing cranial ossification and diminishing ventricular volume. These mice had an intermediate weight gain compared to PO injected SMA animals (Fig. 9A). Median survival was also modestly improved (41±14.2 days, max 79, Log Rank $p<0.001$) (Fig. 9B). Pairwise survival comparison between P0 and P4 treated animals was also

significant (Log Rank p<0.006). Thus, early administration of MO is more effective than late. This will be an important consideration when moving forward towards human clinical applications (37, 68).

We also performed a P4 peripheral vascular injection (50 µg/g, facial vein) of MO into a group of SMA animals. This group of mice (n=9) had decreased survival compared to the P4 ICV injected cohort (21+/-0.354 days, Log Rank p<0.014) (Fig. 9C). We surmise that the later age coupled with less direct targeting of the CNS motor neurons over a shortened period of time (shorter therapeutic window) resulted in greater motor neuron death. This condition argues for the early CNS delivery of bare ASOs for SMA motor neuron targeting.

Discussion

A single nucleotide alteration within exon 7 differentiates *SMN1* and *SMN2* capacity for full-length SMN protein production. Exon 7 exclusion, as a result of modulation of *SMN2* mRNA splicing (5-10), yields a truncated SMN that does not oligomerize efficiently, is unstable and rapidly degraded (11-13). SMN functions in ensuring accurate assembly of Sm proteins onto snRNA. This function is altered in SMA animals (19, 29) in direct correlation with disease severity and altered SnRNP profiles (29, 30). However, assembly of other RNP complexes could also be altered, and SMN has been found in axons (4, 25). The possibility exists for disruption of additional SMN functions that have not yet been elucidated, and SMA could ultimately be a result of splicing changes, RNA transport defects, or a combination of both. Despite the uncertainty, it is clear that SMA is a disease of a reduced functional component of SMN, and thus increasing SMN at the right time and place is predicted to alter the disease course. Elevating SMN in the postnatal period of SMA mice has a marked impact on phenotype (38, 39, 41, 43, 44, 55, 56). Furthermore, we have shown using an inducible mouse that postnatal induction of SMN yields a dramatic rescue of SMA (37); Lutz *et al* have reported similar results using a different inducible system (68). Removal of SMN induction after 28 days has minimal effect on the neuromuscular system, highlighting the critical window for high SMN requirements during neonatal and juvenile mouse development (37). In agreement with these studies, we have found that SMN induction early (P0) by a single bolus dose of MO successfully modulates SMN2 splicing and results in an impressive impact

on SMNΔ7 SMA survival, whereas delayed delivery (P4) had a diminished impact. These results reiterate the importance of early disease diagnosis and therapy.

Many investigative SMA treatments focus on increasing SMN protein levels. Three strategies include compounds that activate the *SMN2* promoter (38-40) (40), transfection of the motor neuron with an SMN producing viral vector (43, 44, 69), and injection of short sequence ASOs that promote modulation of splicing and inclusion of *SMN2* exon 7 (53, 55). There are several chemistries of ASOs, including 2'-OMe, MOE, PNA, and morpholinos that have been used to modify RNA processing in neuromuscular disease (45-47). Multiple groups have published results of CNS ASO injection in mouse models of SMA, and all have shown *SMN2* splice modulation with targeting of ISS-N1 and flanking sequences within intron 7, affirming this region as a strong modulator of exon 7 splice dynamics (45, 48, 53-56). The principle drawback of many of these studies is the relatively mild SMA phenotypic alteration. Williams *et al* used a 2'-OMe ASO and noted an increased animal mass that declined by P12 animal sacrifice, as well as improvement in righting ability (48). The study was complicated by multiple cranial injections on successive days, a possible confounder for animal decline. Hua *et al.* in 2010 compared 2'-OMe and MOE oligomers targeting HSMN2Ex7D(-10 to -27) and found the former substantially less effective (53). 2'-OMe ASO is likely suboptimal in the treatment of SMA mice when used for negative regulator blocking, though it may work well when enhancing positive regulator binding.

Baughan *et al* used a bifunctional 2'-OMe ASO that targeted both an intron 6 negative regulator and attracted SR proteins, thereby enhancing exon 7 incorporation (45). Phenotypic advantage was again modest, although the authors used a more severe model of SMA (*Smn-/-, SMN2+/+*), and thus head-to-head comparison is difficult. Hua *et al* showed that an ICV injected MOE oligomer against ISS-N1 altered necrosis phenotypes in SMN deficient mice that do not show a clear SMA motor phenotype (53). Recently, Passini *et al* (55), using this same MOE, showed improved muscle physiology as well as survival (median of 26 days, 4 μg dose) after ICV treatment in the SMNΔ7 SMA model. This study showed suspected MOE toxicity at doses >8 μg (1.16mM). The authors reported on decay rates and longitudinal splicing changes with their most efficacious ICV bolus dose of 4 μg. The MOE decreased from an apex of 8-10 μg/g in cervical tissue to 2 μg/g

of tissue at P16, and SMN2 splicing was effected at day 3 and 16 but returned to baseline levels by day 30. Due to little if any toxicity demonstrated by bolus CNS dosing of MO, we were able to administer up to 135 μg/day, and 405 μg from P0-3 without adverse effect, and measured *SMN2* splicing changes after single P0 bolus of 81 μg through day 65. Therefore, the reduced CNS toxicity of morpholinos may allow for higher early dosing and achievement of more prolonged splicing modulation.

While the current paper was under review Hua *et al*. reported the results of MOE injection targeting ISS-N1, and also explored various routes of delivery as well as elevated and intermittent dosing strategies (56). These experiments used a different mouse model of SMA developed by Hsieh-Li *et al.* (34), which is characterized by mouse Smn lacking exon 7, thus producing a truncated transcript, as well as two copies of *SMN2* on a chromosome. Mice live for an average of 10-11 days and display a similar phenotype to the SMNΔ7 SMA animals. Despite many similarities, it is possible that there is unique tissue variability in *SMN2* expression between these two SMA models. Nevertheless, the authors found minor survival advantage after a single P0 MOE ICV bolus dose of 20 μg (2.9mM, 16 vs. 10 days). This dose is comparable to our 27 μg dose and resultant median survival of 83 days. It is possible that morpholinos have a longer half-life within the CNS and thus a longer duration of effect.

Hua *et al.* reported long survival after multiple peripheral doses (median 137 days), and conclude that peripheral SMN restoration is essential for SMA treatment. *SMN2* splicing was modulated at high levels in both the periphery (liver, heart, kidney, muscle) and in the CNS (brain and spine) after peripheral delivery. It is important to consider the pharmacokinetics of single versus multiple dosing, such that the latter would result in a more sustained therapeutic window and longer-term splice modulation over the critical early period in SMA. Furthermore, it is clear that both MOEs and morpholinos cross the immature blood-brain-barrier in neonatal mice and modulate CNS splicing, and we suspect that such translocation would not be recapitulated in human infants. We propose that sustained increased levels of CNS SMN throughout a critical early window is essential for SMA therapy, in agreement with previous findings (44, 57, 58).

A morpholino ASO directed against ISS-N1 induces a robust and sustained *SMN2* exon 7 incorporation, leading to unequivocal SMN protein increases in both brain and spinal cord tissue. These findings correlate with an impressive SMNΔ7 SMA survival advantage (max. 161 days, median 112 days, high dose MO). When compared to scAAV9-SMN injection, our weight gain and righting paralleled with these animals, although after viral transfection the investigators had complete survival rescue (44). ICV injection was performed by bolus injection at a single time (P0) or at two time points (P0 and P30) with no difference in survival between the two groups. However, scAAV9-SMN animals were exposed to continuous SMN production due to viral-cell transduction. The morpholino is not immune to either dilution with animal growth or to eventual hepatic or renal clearance, and multiple boluses or continuous MO dosing by intrathecal osmotic pump placed during adolescence may further prolong survival. Alternatively, ICV dosing may miss a critical target such as the extra-CNS autonomic nervous system, though this seems less likely given the lack of increased animal survival over-and-above P0 ICV when ICV was combined with FV dosing.

FV delivered MO at P0 also had long-term survival, though we surmise that the leaky blood-brain-barrier in the immature mouse pup allows for translocation of ASO into the CNS, as demonstrated by ddPCR analysis. MO was also delivered by FV at P4, which resulted in only mild animal rescue, suggesting that the critical target for SMN level modulation resides within the CNS and must be acted on early. It may still be important to increase peripheral SMN, though in a more continuous fashion so as to surmount renal and hepatic clearance, which could be accomplished with multiple intravascular administrations by tail vein injection or indwelling central venous catheter placement.

Despite both increased inclusion of exon 7 in *SMN2* transcript as well as elevated SMN protein levels at delayed time points (P45-65), treated SMA mice developed an interesting and time-predictable phenotype of ear and tail necrosis. This necrosis pattern is not unlike that seen in less severe SMA mouse models (34) or in mice treated with less potent activators of SMN (38). The patterns of necrosis could represent dysfunction in cell populations outside of the CNS that are not fully or continuously exposed to the targeting morpholino delivered by bolus ICV or FV. We have previously shown that high levels of SMN in neurons, but not in muscle, can increase survival of *Smn-/-; SMN2+/+* mice; however, the contribution of extra-neuronal SMN has

not been fully elucidated (57). The necrosis of peripheral structures, together with priapism, urinary retention and bowel obstruction, all serve as clinical evidence supporting potential autonomic nervous system (ANS) dysfunction in SMA. A number of groups have reported cardiac bradyarrythmias, as well as dilated cardiomyopathy coupled with decreased contractility, in SMA mouse models (67, 70, 71), possibly due to a SMN deficient sympathetic nervous system leading to autonomic imbalance. Interestingly, some of our adult MO treated mice died suddenly before showing any evidence of disease morbidity (i.e. weight loss, necrosis); we postulate that such sudden and unpredictable mortality is most likely due to acute cardiopulmonary failure resulting from autonomic dysfunction. There is increasing human clinical evidence of autonomic nervous system imbalance in SMA. Retrospective reports describe an increased incidence of cardiac arrhythmias and wall-motion abnormalities in patients with Type I SMA (72-74). Autonomic testing, including skin vessel vasodilatation response and circulating norepinephrine levels, also suggest autonomic dysfunction (75). Morphologic and functional cardiac evaluation of MO injected mice will help elucidate the contribution of autonomic dysfunction on animal demise.

P0 injection of MO produced a striking increase in survival, delayed ICV injection had intermediate survival, and delayed facial vein injection yielded only mild rescue. These results again imply the importance of early CNS elevations of SMN. (37, 44, 57, 68). Previous examination of neuronal morphology in severe SMA embryos (*Smn-/-, SMN2+/+*) showed decreased synapse occupation by motor axons, suggesting that SMN is a critical component for early synapse development and maturation (28). Temporal induction of SMN in SMA mice has defined a window of increased SMN production for correction of the SMA phenotype in mice (37, 68). Therefore, a period during neonatal growth in the mouse constitutes a critical time for high SMN production. It is increasingly clear that any potential SMA therapeutic will have maximum effect when given as early as possible.

Strategies for increasing SMN and altering the course of SMA are proliferating, including ASOs, viral therapy with ScAAV9-SMN, and drug compounds that induce SMN. The latter modality has the simplicity of application and the ability to ensure target levels within tissue. Drawbacks include non-specific targeting and resultant potential toxicity. Viral therapy has the distinct advantage of having the longest laboratory survival

increase of all interventions and the need for only a single vascular delivery (44). Disadvantages include the hurdles of large-scale production, as well as a patient subpopulation that is seropositive for the AAV9 capsid. ASOs are maturing as potential disease modifiers in SMA and other neuromuscular disease. Morpholinos have notable efficacy through exon skipping in Duchenne muscular dystrophy (46, 49), showing low toxicity, high specificity, and excellent body-wide distribution after systemic administration (46, 60, 61, 63, 76). Disadvantages of ASO therapy for SMA include the probability of invasive repeat CNS dosing.

Our study has shown that a single CNS bolus of morpholino targeting ISS-N1 of *SMN2* can strongly modulate splicing mechanics, increase SMN protein and increase survival of SMNΔ7 SMA mice to a greater extent than other previously trialed ASO chemistries. Furthermore, morpholinos appear to have little or no toxicity when delivered at high doses within the CNS. This therapy has the potential for translation into clinical trials with early administration of MO via intrathecal delivery.

Continued refinement of dosing (when, where, how much?) should continue in order to optimize delivery for future clinical trials. A large animal model of SMA, such as the pig, could be used to both titrate the optimal dosing and to truly evaluate the efficacy of peripherally administered ASO therapy for SMA in the setting of an intact blood-brain-barrier. It is clear that earlier correction of SMN protein levels has more profound effects than delayed increases, emphasizing the importance of early SMA detection and intervention in future clinical trial design. Methods of newborn SMA detection have been developed but implementation presents complications (77), including whether an SMA therapy must first demonstrate efficacy in symptomatic patients before the start of widespread newborn screening. We believe that new data showing both profound disease modification with therapy, as well as the clear advantage of pre-morbid treatment initiation, advocates for the start of SMA neonatal screening.

Materials and Methods

Generation of SMA Mice: SMNΔ7 carrier breeding mice (*SMN2+/+; Smn+/-;* SMNΔ7*+/+*) were crossed to generate three types of offspring varying in mouse *Smn* genotype: *Smn +/+*, *Smn +/-* and *Smn -/-* as previously described (36, 39). All breeding and subsequent use of animals in this study where approved by the IACUC of

The Ohio State University, Columbus, Ohio.

ICV injections: The P0 or P4 pup was cryo-anesthetized and hand-mounted over a back-light to visualize the intersection of the coronal and sagittal cranial sutures (*bregma*) (55, 58). A fine-drawn capillary needle with injection assembly was inserted 1 mm lateral and 1 mm posterior to *bregma*, and then tunneled 1mm deep to the skin edge (approximating) ipsilateral lateral ventricle. An opaque tracer (Evans blue, 0.04%) was added to the reagent to visualize the borders of the lateral ventricle after injection of 2μl of morpholino.

Stereotactic injections: P30 mice were anesthetized with inhalational isoflurane (3% induction, maintenance 1% mixed with high-flow 100% O2). The animal was placed into the cranial stereotactic frame (Kopf Instruments) with digital coordinate guidance (myNeuroLab), and the anesthesia nose cone was secured. The cranial apex was sterilized and a short midline incision was performed with visualization of *bregma* and *lambda*. A small burr hole was drilled and cranial needle with attached Hamilton syringe was guided to preselected coordinates (A/P 0.58mm, D/L 2.15mm, M/L 1.10mm) for right lateral ventricle cannulation (78), the coordinates were validated by injection of scAAV4-GFP (ependymal localization, Fig. S3) in a trial P30 mouse. 18цg/g of MO or scMO (equivalent to low dose (2mM) injection in the P0 pups) was injected at a rate of 0.75цL/min with digital microinjector (KD Scientific). After injection, the needle was withdrawn and skin closed with running suture. Post-surgical care was approved by the IACUC of The Ohio State University, Columbus, Ohio.

Facial Vein Injection: Facial vein injection on P0 pups was performed as previously described (79). Mo or scMO was dosed at 50цg/g body mass.

Mouse Genotyping: The *SMN2*, *Smn* knockout allele and SMNΔ7 alleles were genotyped as previously described (36, 44, 57). Tail snips were gathered at P0, each pup was identified by paw tattooing. All genotyping was performed on P0 as described previously (44).

Behavioral analysis: All injected animals, as well as breeding pairs, were monitored each day for morbidity, mortality, and new litters. Control and experimental animals were weighed each day, and righting response was assessed during the animals' first 21 days as previously described (80). Grip strength was recorded as previously described with correction for the weight of the animals (81).

RT-PCR and Real-Time RT-PCR analysis: RNA was isolated from Trizol (Invitrogen) homogenized tissue and purified with the RNeasy kit (Qiagen). RT-PCR was performed as previously described (57). The SMNΔ7 transgene lacks the terminal portion of exon 8. Primers were designed to amplify only the *SMN2* transcripts that contain this region, thus distinguishing SMNΔ7 from *SMN2*: (hSMN2E8rev) TTATATACTTTTAAACATATAGAAGATAG, (hSMNE6fwd) AGATTCTCTTGATGATGCTGAATG.

Real-time RT-PCR assayed for full-length SMN2 transcripts relative to cyclophilin. *SMN2* amplification: (hSMNFull Fb) GTTTCAGACAAAATCAAAAAGAAGGA, (hSMNFull Rc) TCTATAACGCTTCACATTCCAGATCT, probe: (hSMNFull FAM) ATGCCAGCATTTCTCCTTAATTTAAGG. Cyclophilin: (QcycloF) GTCAACCCCACCGTGTTCTT, (QcycloR) TTGGAACTTTGTCTGCAAACA, probe: (Probecyclo NED) CTTGGGCCGCGTCT. PCR reaction for *SMN2* used 2 μl cDNA, 0.6 μl (300nm) forward and reverse primer; cyclophilin, 1.8 μl (900nM) forward and reverse primer. Transcript level was determined as previously described (82).

Digital Droplet PCR: cDNA was collected as detailed above. Identical primers and probe were used for ddPCR as was used for real time RT-PCR. The PCR reaction for *SMN2* used 1.0 μl cDNA and cyclophilin used 0.1 μl. 1.8 μl (900nm) forward and reverse primer was used for both *SMN2* and cyclophilin. Droplet

generation and reader analysis were performed on QuantaLife (www.quantalife.com/, now Bio-Rad) hardware. Ten to fifteen thousand droplets containing cDNA transcript and PCR reagents were generated before amplification. Transcript concentration was first calculated by the droplet reader using poisson statistical distributions (65), and relative SMN2 levels were determined by calculating the ratio of *SMN2* versus cyclophilin.

Western: Western blot analysis was performed as previously described (36, 37, 57). Detection was performed using the LI-COR Odyssey Imaging System (Biosciences) and quantification was determined using Odyssey Infrared Imaging System Application Software (Biosciences).

Morpholino ASO Preparation: The MO sequence, numbered from the *SMN2* exon 7 donor site (Figure 1), was ATTCACTTTCATAATGCTGG (MWT=6754, Gene Tools). scMO sequence was TCCTTTAAAGTATTGTGACC (MWT=6754, Gene Tools). Morpholinos were resuspended in sterile 0.9% sodium chloride, aliquoted, and mixed with Evans Blue (final concentration 0.04%). Three different molar concentrations were prepared (High: 6mM=40.5μg/μL; Middle: 4mM=27μg/μL; Low: 2mM =13.5μg/μL). Stock solutions were stored at -20^{o}C, working solutions at 4^{o}C. Lissamine tagged morpholino (sequence CCTCTTACCTCAGTTACAATTTATA) was resuspended to 2mM in 0.9% NaCl. 2μl of morpholino oligomer was injected, yielding total doses per animal of 81μg (High), 54μg (Middle) and 27μg (Low).

SMN Immunofluorescence: SMNΔ7 SMA mice (*SMN2*+/+; HB9:GFP; *Smn*-/-; SMNΔ7*+/+)* were injected by P0 ICV with 4mM MO. Carrier control was not injected. Spinal cords were harvested, frozen, fixed and sectioned at P7 as previously described (37). Tissue sections were stained with anti-human SMN KH antibody 1:10 overnight and Alexa Fluor® 594 goat anti-rabbit IgG (Molecular probes) (1:1000). Endogenous lissamine (RFP) and GFP fluorescence were imaged with a Nikon E800 Eclipse fluorescent microscope, Ultrapix Digital Camera (Olympus) with MagnaFIRE v2.1C software (Optronics), and further processed with Adobe Photoshop

CS2.

Statistical Analysis:

Data are expressed as means+/- standard errors. Kaplan-Meier curves were generated from the survival data and tested using the Mantel-Cox log rank test. All statistical analyses were performed with SPSS v.16.0.

Funding

This work was supported by the National Institutes of Health R01 HD060586 (AHMB) and RC2 NS069476 (AHMB); The Ohio State University Department of Neurological Surgery (PNP); AFM/SMA Europe (SW), the Spinal Muscular Atrophy Association of Australia (SW) and the Parry Foundation of Australia (SW).

Acknowledgements

We thank Dr. Yimin Hua and Dr. Adrian Krainer for the generous gift of human specific KH SMN antibody and interesting discussions, as well as Aurelie Massoni-Laporte for help on real time RT-PCR primer design and use.

References

1 Roberts, D.F., Chavez, J. and Court, S.D. (1970) The genetic component in child mortality. *Arch. Dis. Child.*, **45**, 33-38.

2 Crawford, T.O. and Pardo, C.A. (1996) The neurobiology of childhood spinal muscular atrophy. *Neurobiol. Dis.*, **3**, 97-110.

3 Lefebvre, S., Burglen, L., Reboullet, S., Clermont, O., Burlet, P., Viollet, L., Benichou, B., Cruaud, C., Millasseau, P., Zeviani, M. *et al.* (1995) Identification and characterization of a spinal muscular atrophy-determining gene. *Cell*, **80**, 155-165.

4 Burghes, A.H. and Beattie, C.E. (2009) Spinal muscular atrophy: why do low levels of survival motor neuron protein make motor neurons sick? *Nat. Rev. Neurosci.*, **10**, 597-609.

5 Parsons, D.W., McAndrew, P.E., Monani, U.R., Mendell, J.R., Burghes, A.H. and Prior, T.W. (1996) An 11 base pair duplication in exon 6 of the SMN gene produces a type I spinal muscular atrophy (SMA) phenotype: further evidence for SMN as the primary SMA-determining gene. *Hum. Mol. Genet.*, **5**, 1727-1732.

6 Kashima, T. and Manley, J.L. (2003) A negative element in SMN2 exon 7 inhibits splicing in spinal muscular atrophy. *Nat. Genet.*, **34**, 460-463.

7 Monani, U.R., Lorson, C.L., Parsons, D.W., Prior, T.W., Androphy, E.J., Burghes, A.H. and McPherson, J.D. (1999) A single nucleotide difference that alters splicing patterns distinguishes the SMA gene SMN1 from the copy gene SMN2. *Hum. Mol. Genet.*, **8**, 1177-1183.

8 Lorson, C.L., Hahnen, E., Androphy, E.J. and Wirth, B. (1999) A single nucleotide in the SMN gene regulates splicing and is responsible for spinal muscular atrophy. *Proc. Natl. Acad. Sci. U S A.*, **96**, 6307-6311.

9 Cartegni, L. and Krainer, A.R. (2002) Disruption of an SF2/ASF-dependent exonic splicing enhancer in SMN2 causes spinal muscular atrophy in the absence of SMN1. *Nat. Genet.*, **30**, 377-384.

10 Gennarelli, M., Lucarelli, M., Capon, F., Pizzuti, A., Merlini, L., Angelini, C., Novelli, G. and Dallapiccola, B. (1995) Survival motor neuron gene transcript analysis in muscles from spinal muscular atrophy patients. *Biochem Biophys Res. Commun.*, **213**, 342-348.

11 Burnett, B.G., Munoz, E., Tandon, A., Kwon, D.Y., Sumner, C.J. and Fischbeck, K.H. (2009) Regulation of SMN protein stability. *Mol. Cell Biol.*, **29**, 1107-1115.

12 Lorson, C.L., Strasswimmer, J., Yao, J.M., Baleja, J.D., Hahnen, E., Wirth, B., Le, T., Burghes, A.H. and Androphy, E.J. (1998) SMN oligomerization defect correlates with spinal muscular atrophy severity. *Nat. Genet.*, **19**, 63-66.

13 Lorson, C.L. and Androphy, E.J. (2000) An exonic enhancer is required for inclusion of an essential exon in the SMA-determining gene SMN. *Hum. Mol. Genet.*, **9**, 259-265.

14 Burghes, A.H. (1997) When is a deletion not a deletion? When it is converted. *Am. J. Hum. Genet.*, **61**, 9-15.

15 McAndrew, P.E., Parsons, D.W., Simard, L.R., Rochette, C., Ray, P.N., Mendell, J.R., Prior, T.W. and Burghes, A.H. (1997) Identification of proximal spinal muscular atrophy carriers and patients by analysis of SMNT and SMNC gene copy number. *Am. J. Hum. Genet.*, **60**, 1411-1422.

16 Prior, T.W., Krainer, A.R., Hua, Y., Swoboda, K.J., Snyder, P.C., Bridgeman, S.J., Burghes, A.H. and Kissel, J.T. (2009) A positive modifier of spinal muscular atrophy in the SMN2 gene. *Am. J. Hum. Genet.*, **85**, 408-413.

17 Vezain, M., Saugier-Veber, P., Goina, E., Touraine, R., Manel, V., Toutain, A., Fehrenbach, S., Frebourg, T., Pagani, F., Tosi, M. *et al.* (2010) A rare SMN2 variant in a previously unrecognized composite splicing regulatory element induces exon 7 inclusion and reduces the clinical severity of spinal muscular atrophy. *Hum. Mutat.*, **31**, E1110-1125.

18 Sun, Y., Grimmler, M., Schwarzer, V., Schoenen, F., Fischer, U. and Wirth, B. (2005) Molecular and functional analysis of intragenic SMN1 mutations in patients with spinal muscular atrophy. *Hum. Mutat.*, **25**, 64-71.
19 Workman, E., Saieva, L., Carrel, T.L., Crawford, T.O., Liu, D., Lutz, C., Beattie, C.E., Pellizzoni, L. and Burghes, A.H. (2009) A SMN missense mutation complements SMN2 restoring snRNPs and rescuing SMA mice. *Hum. Mol. Genet.*, **18**, 2215-2229.
20 Meister, G., Buhler, D., Pillai, R., Lottspeich, F. and Fischer, U. (2001) A multiprotein complex mediates the ATP-dependent assembly of spliceosomal U snRNPs. *Nat. Cell Biol.*, **3**, 945-949.
21 Pellizzoni, L., Yong, J. and Dreyfuss, G. (2002) Essential role for the SMN complex in the specificity of snRNP assembly. *Science*, **298**, 1775-1779.
22 Pellizzoni, L. (2007) Chaperoning ribonucleoprotein biogenesis in health and disease. *EMBO Rep*, **8**, 340-345.
23 Schrank, B., Gotz, R., Gunnersen, J.M., Ure, J.M., Toyka, K.V., Smith, A.G. and Sendtner, M. (1997) Inactivation of the survival motor neuron gene, a candidate gene for human spinal muscular atrophy, leads to massive cell death in early mouse embryos. *Proc. Natl. Acad. Sci. U S A.*, **94**, 9920-9925.
24 Rossoll, W., Kroning, A.K., Ohndorf, U.M., Steegborn, C., Jablonka, S. and Sendtner, M. (2002) Specific interaction of Smn, the spinal muscular atrophy determining gene product, with hnRNP-R and gry-rbp/hnRNP-Q: a role for Smn in RNA processing in motor axons? *Hum. Mol. Genet.*, **11**, 93-105.
25 Rossoll, W., Jablonka, S., Andreassi, C., Kroning, A.K., Karle, K., Monani, U.R. and Sendtner, M. (2003) Smn, the spinal muscular atrophy-determining gene product, modulates axon growth and localization of beta-actin mRNA in growth cones of motoneurons. *J. Cell Biol.*, **163**, 801-812.
26 McWhorter, M.L., Monani, U.R., Burghes, A.H. and Beattie, C.E. (2003) Knockdown of the survival motor neuron (Smn) protein in zebrafish causes defects in motor axon outgrowth and pathfinding. *J. Cell Biol.*, **162**, 919-931.
27 Carrel, T.L., McWhorter, M.L., Workman, E., Zhang, H., Wolstencroft, E.C., Lorson, C., Bassell, G.J., Burghes, A.H. and Beattie, C.E. (2006) Survival motor neuron function in motor axons is independent of functions required for small nuclear ribonucleoprotein biogenesis. *J. Neurosci.*, **26**, 11014-11022.
28 McGovern, V.L., Gavrilina, T.O., Beattie, C.E. and Burghes, A.H. (2008) Embryonic motor axon development in the severe SMA mouse. *Hum. Mol. Genet.*, **17**, 2900-2909.
29 Gabanella, F., Butchbach, M.E., Saieva, L., Carissimi, C., Burghes, A.H. and Pellizzoni, L. (2007) Ribonucleoprotein assembly defects correlate with spinal muscular atrophy severity and preferentially affect a subset of spliceosomal snRNPs. *PLoS One*, **2**, e921.
30 Zhang, Z., Lotti, F., Dittmar, K., Younis, I., Wan, L., Kasim, M. and Dreyfuss, G. (2008) SMN deficiency causes tissue-specific perturbations in the repertoire of snRNAs and widespread defects in splicing. *Cell*, **133**, 585-600.
31 Baumer, D., Lee, S., Nicholson, G., Davies, J.L., Parkinson, N.J., Murray, L.M., Gillingwater, T.H., Ansorge, O., Davies, K.E. and Talbot, K. (2009) Alternative splicing events are a late feature of pathology in a mouse model of spinal muscular atrophy. *PLoS Genet*, **5**, e1000773.
32 Coovert, D.D., Le, T.T., McAndrew, P.E., Strasswimmer, J., Crawford, T.O., Mendell, J.R., Coulson, S.E., Androphy, E.J., Prior, T.W. and Burghes, A.H. (1997) The survival motor neuron protein in spinal muscular atrophy. *Hum. Mol. Genet.*, **6**, 1205-1214.
33 Lefebvre, S., Burlet, P., Liu, Q., Bertrandy, S., Clermont, O., Munnich, A., Dreyfuss, G. and Melki, J. (1997) Correlation between severity and SMN protein level in spinal muscular atrophy. *Nat. Genet.*, **16**, 265-269.
34 Hsieh-Li, H.M., Chang, J.G., Jong, Y.J., Wu, M.H., Wang, N.M., Tsai, C.H. and Li, H. (2000) A mouse model for spinal muscular atrophy. *Nat. Genet.*, **24**, 66-70.

35 Monani, U.R., Sendtner, M., Coovert, D.D., Parsons, D.W., Andreassi, C., Le, T.T., Jablonka, S., Schrank, B., Rossoll, W., Prior, T.W. *et al.* (2000) The human centromeric survival motor neuron gene (SMN2) rescues embryonic lethality in Smn(-/-) mice and results in a mouse with spinal muscular atrophy. *Hum. Mol. Genet.*, **9**, 333-339.
36 Le, T.T., Pham, L.T., Butchbach, M.E., Zhang, H.L., Monani, U.R., Coovert, D.D., Gavrilina, T.O., Xing, L., Bassell, G.J. and Burghes, A.H. (2005) SMNDelta7, the major product of the centromeric survival motor neuron (SMN2) gene, extends survival in mice with spinal muscular atrophy and associates with full-length SMN. *Hum. Mol. Genet.*, **14**, 845-857.
37 Le, T.T., McGovern, V.L., Alwine, I.E., Wang, X., Massoni-Laporte, A., Rich, M.M. and Burghes, A.H. (2011) Temporal requirement for high SMN expression in SMA mice. *Hum. Mol. Genet.*, **20**, 3578-3591.
38 Avila, A.M., Burnett, B.G., Taye, A.A., Gabanella, F., Knight, M.A., Hartenstein, P., Cizman, Z., Di Prospero, N.A., Pellizzoni, L., Fischbeck, K.H. *et al.* (2007) Trichostatin A increases SMN expression and survival in a mouse model of spinal muscular atrophy. *J. Clin. Invest.*, **117**, 659-671.
39 Butchbach, M.E., Singh, J., Thorsteinsdottir, M., Saieva, L., Slominski, E., Thurmond, J., Andresson, T., Zhang, J., Edwards, J.D., Simard, L.R. *et al.* (2010) Effects of 2,4-diaminoquinazoline derivatives on SMN expression and phenotype in a mouse model for spinal muscular atrophy. *Hum. Mol. Genet.*, **19**, 454-467.
40 Farooq, F., Molina, F.A., Hadwen, J., Mackenzie, D., Witherspoon, L., Osmond, M., Holcik, M. and Mackenzie, A. (2011) Prolactin increases SMN expression and survival in a mouse model of severe spinal muscular atrophy via the STAT5 pathway. *J. Clin. Invest.*, **121**, 3042-3050.
41 Hastings, M.L., Berniac, J., Liu, Y.H., Abato, P., Jodelka, F.M., Barthel, L., Kumar, S., Dudley, C., Nelson, M., Larson, K. *et al.* (2009) Tetracyclines that promote SMN2 exon 7 splicing as therapeutics for spinal muscular atrophy. *Sci. Transl. Med.*, **1**, 5ra12.
42 Dominguez, E., Marais, T., Chatauret, N., Benkhelifa-Ziyyat, S., Duque, S., Ravassard, P., Carcenac, R., Astord, S., Pereira de Moura, A., Voit, T. *et al.* Intravenous scAAV9 delivery of a codon-optimized SMN1 sequence rescues SMA mice. *Hum. Mol. Genet.*, **20**, 681-693.
43 Valori, C.F., Ning, K., Wyles, M., Mead, R.J., Grierson, A.J., Shaw, P.J. and Azzouz, M. (2010) Systemic delivery of scAAV9 expressing SMN prolongs survival in a model of spinal muscular atrophy. *Sci. Transl. Med.*, **2**, 35ra42.
44 Foust, K.D., Wang, X., McGovern, V.L., Braun, L., Bevan, A.K., Haidet, A.M., Le, T.T., Morales, P.R., Rich, M.M., Burghes, A.H. *et al.* (2010) Rescue of the spinal muscular atrophy phenotype in a mouse model by early postnatal delivery of SMN. *Nat. Biotechnol.*, **28**, 271-274.
45 Baughan, T.D., Dickson, A., Osman, E.Y. and Lorson, C.L. (2009) Delivery of bifunctional RNAs that target an intronic repressor and increase SMN levels in an animal model of spinal muscular atrophy. *Hum. Mol. Genet.*, **18**, 1600-1611.
46 Wilton, S.D., Lloyd, F., Carville, K., Fletcher, S., Honeyman, K., Agrawal, S. and Kole, R. (1999) Specific removal of the nonsense mutation from the mdx dystrophin mRNA using antisense oligonucleotides. *Neuromuscul. Disord.*, **9**, 330-338.
47 Burghes, A.H. and McGovern, V.L. (2010) Antisense oligonucleotides and spinal muscular atrophy: skipping along. *Genes Dev.*, **24**, 1574-1579.
48 Williams, J.H., Schray, R.C., Patterson, C.A., Ayitey, S.O., Tallent, M.K. and Lutz, G.J. (2009) Oligonucleotide-mediated survival of motor neuron protein expression in CNS improves phenotype in a mouse model of spinal muscular atrophy. *J. Neurosci.*, **29**, 7633-7638.
49 Alter, J., Lou, F., Rabinowitz, A., Yin, H., Rosenfeld, J., Wilton, S.D., Partridge, T.A. and Lu, Q.L. (2006) Systemic delivery of morpholino oligonucleotide restores dystrophin expression bodywide and improves dystrophic pathology. *Nat. Med.*, **12**, 175-177.

50 Morcos, P.A. (2007) Achieving targeted and quantifiable alteration of mRNA splicing with Morpholino oligos. *Biochem. Biophys. Res. Commun.*, **358**, 521-527.
51 Bebee, T.W., Gladman, J.T. and Chandler, D.S. (2011) Splicing regulation of the survival motor neuron genes and implications for treatment of spinal muscular atrophy. *Front Biosci.*, **15**, 1191-1204.
52 Singh, N.K., Singh, N.N., Androphy, E.J. and Singh, R.N. (2006) Splicing of a critical exon of human Survival Motor Neuron is regulated by a unique silencer element located in the last intron. *Mol. Cell Biol.*, **26**, 1333-1346.
53 Hua, Y., Sahashi, K., Hung, G., Rigo, F., Passini, M.A., Bennett, C.F. and Krainer, A.R. (2010) Antisense correction of SMN2 splicing in the CNS rescues necrosis in a type III SMA mouse model. *Genes Dev.*, **24**, 1634-1644.
54 Hua, Y., Vickers, T.A., Okunola, H.L., Bennett, C.F. and Krainer, A.R. (2008) Antisense masking of an hnRNP A1/A2 intronic splicing silencer corrects SMN2 splicing in transgenic mice. *Am. J. Hum. Genet.*, **82**, 834-848.
55 Passini, M.A., Bu, J., Richards, A.M., Kinnecom, C., Sardi, S.P., Stanek, L.M., Hua, Y., Rigo, F., Matson, J., Hung, G. *et al.* (2011) Antisense oligonucleotides delivered to the mouse CNS ameliorate symptoms of severe spinal muscular atrophy. *Sci. Transl. Med.*, **3**, 72ra18.
56 Hua, Y., Sahashi, K., Rigo, F., Hung, G., Horev, G., Bennett, C.F. and Krainer, A.R. (2011) Peripheral SMN restoration is essential for long-term rescue of a severe spinal muscular atrophy mouse model. *Nature*, **478**, 123-126.
57 Gavrilina, T.O., McGovern, V.L., Workman, E., Crawford, T.O., Gogliotti, R.G., DiDonato, C.J., Monani, U.R., Morris, G.E. and Burghes, A.H. (2008) Neuronal SMN expression corrects spinal muscular atrophy in severe SMA mice while muscle-specific SMN expression has no phenotypic effect. *Hum. Mol. Genet.*, **17**, 1063-1075.
58 Passini, M.A., Bu, J., Roskelley, E.M., Richards, A.M., Sardi, S.P., O'Riordan, C.R., Klinger, K.W., Shihabuddin, L.S. and Cheng, S.H. (2010) CNS-targeted gene therapy improves survival and motor function in a mouse model of spinal muscular atrophy. *J. Clin. Invest.*, **120**, 1253-1264.
59 Ellett, F. and Lieschke, G.J. (2010) Zebrafish as a model for vertebrate hematopoiesis. *Curr. Opin. Pharmacol.*, **10**, 563-570.
60 Wu, B., Xiao, B., Cloer, C., Shaban, M., Sali, A., Lu, P., Li, J., Nagaraju, K., Xiao, X. and Lu, Q.L. (2011) One-year treatment of morpholino antisense oligomer improves skeletal and cardiac muscle functions in dystrophic mdx mice. *Mol. Ther.*, **19**, 576-583.
61 Yokota, T., Lu, Q.L., Partridge, T., Kobayashi, M., Nakamura, A., Takeda, S. and Hoffman, E. (2009) Efficacy of systemic morpholino exon-skipping in Duchenne dystrophy dogs. *Ann Neurol.*, **65**, 667-676.
62 Kinali, M., Arechavala-Gomeza, V., Feng, L., Cirak, S., Hunt, D., Adkin, C., Guglieri, M., Ashton, E., Abbs, S., Nihoyannopoulos, P. *et al.* (2009) Local restoration of dystrophin expression with the morpholino oligomer AVI-4658 in Duchenne muscular dystrophy: a single-blind, placebo-controlled, dose-escalation, proof-of-concept study. *Lancet Neurol*, **8**, 918-928.
63 Cirak, S., Arechavala-Gomeza, V., Guglieri, M., Feng, L., Torelli, S., Anthony, K., Abbs, S., Garralda, M.E., Bourke, J., Wells, D.J. *et al.* (2011) Exon skipping and dystrophin restoration in patients with Duchenne muscular dystrophy after systemic phosphorodiamidate morpholino oligomer treatment: an open-label, phase 2, dose-escalation study. *Lancet*, **378**, 595-605.
64 Sazani, P., Van Ness, K.P., Weller, D.L., Poage, D.W., Palyada, K. and Shrewsbury, S.B. (2011) Repeat-Dose Toxicology Evaluation in Cynomolgus Monkeys of AVI-4658, a Phosphorodiamidate Morpholino Oligomer (PMO) Drug for the Treatment of Duchenne Muscular Dystrophy. *Int. J. Toxicol.*, **30**, 313-321.

65 Zhong, Q., Bhattacharya, S., Kotsopoulos, S., Olson, J., Taly, V., Griffiths, A.D., Link, D.R. and Larson, J.W. (2011) Multiplex digital PCR: breaking the one target per color barrier of quantitative PCR. *Lab on a chip*, **11**, 2167-2174.
66 Wichterle, H., Lieberam, I., Porter, J.A. and Jessell, T.M. (2002) Directed differentiation of embryonic stem cells into motor neurons. *Cell*, **110**, 385-397.
67 Bevan, A.K., Hutchinson, K.R., Foust, K.D., Braun, L., McGovern, V.L., Schmelzer, L., Ward, J.G., Petruska, J.C., Lucchesi, P.A., Burghes, A.H. *et al.* (2010) Early heart failure in the SMN{Delta}7 model of spinal muscular atrophy and correction by postnatal scAAV9-SMN delivery. *Hum. Mol. Genet.*, **19**, 3895-3905.
68 Lutz, C.M., Kariya, S., Patruni, S., Osborne, M.A., Liu, D., Henderson, C.E., Li, D.K., Pellizzoni, L., Rojas, J., Valenzuela, D.M. *et al.* (2011) Postsymptomatic restoration of SMN rescues the disease phenotype in a mouse model of severe spinal muscular atrophy. *J. Clin. Invest.*, **121**, 3029-3041.
69 Dominguez, E., Marais, T., Chatauret, N., Benkhelifa-Ziyyat, S., Duque, S., Ravassard, P., Carcenac, R., Astord, S., de Moura, A.P., Voit, T. *et al.* (2011) Intravenous scAAV9 delivery of a codon-optimized SMN1 sequence rescues SMA mice. *Hum. Mol. Genet.*, **20**, 681-693.
70 Heier, C.R., Satta, R., Lutz, C. and DiDonato, C.J. (2010) Arrhythmia and cardiac defects are a feature of spinal muscular atrophy model mice. *Hum. Mol. Genet.*, **19**, 3906-3918.
71 Shababi, M., Habibi, J., Yang, H.T., Vale, S.M., Sewell, W.A. and Lorson, C.L. (2010) Cardiac defects contribute to the pathology of spinal muscular atrophy models. *Hum. Mol. Genet.*, **19**, 4059-4071.
72 Bach, J.R. (2007) Medical considerations of long-term survival of Werdnig-Hoffmann disease. *Am. J. Phys. Med. Rehabil.*, **86**, 349-355.
73 Hachiya, Y., Arai, H., Hayashi, M., Kumada, S., Furushima, W., Ohtsuka, E., Ito, Y., Uchiyama, A. and Kurata, K. (2005) Autonomic dysfunction in cases of spinal muscular atrophy type 1 with long survival. *Brain Dev.*, **27**, 574-578.
74 Finsterer, J. and Stollberger, C. (1999) Cardiac involvement in Werdnig-Hoffmann's spinal muscular atrophy. *Cardiology*, **92**, 178-182.
75 Arai, H., Tanabe, Y., Hachiya, Y., Otsuka, E., Kumada, S., Furushima, W., Kohyama, J., Yamashita, S., Takanashi, J. and Kohno, Y. (2005) Finger cold-induced vasodilatation, sympathetic skin response, and R-R interval variation in patients with progressive spinal muscular atrophy. *J. Child Neurol.*, **20**, 871-875.
76 Wu, B., Benrashid, E., Lu, P., Cloer, C., Zillmer, A., Shaban, M. and Lu, Q.L. (2011) Targeted skipping of human dystrophin exons in transgenic mouse model systemically for antisense drug development. *PLoS ONE*, **6**, e19906.
77 Prior, T.W., Snyder, P.J., Rink, B.D., Pearl, D.K., Pyatt, R.E., Mihal, D.C., Conlan, T., Schmalz, B., Montgomery, L., Ziegler, K. *et al.* (2010) Newborn and carrier screening for spinal muscular atrophy. *Am. J. Med. Genet. A.*, **152A**, 1608-1616.
78 Paxinos, G. and Franklin, K.B.J. (2004) *The Mouse Brain in Stereotactic Coordinates: Compact Second Edition, Second Edition*. Elsevier Science, USA.
79 Foust, K.D., Nurre, E., Montgomery, C.L., Hernandez, A., Chan, C.M. and Kaspar, B.K. (2009) Intravascular AAV9 preferentially targets neonatal neurons and adult astrocytes. *Nat. Biotechnol.*, **27**, 59-65.
80 Butchbach, M.E., Edwards, J.D. and Burghes, A.H. (2007) Abnormal motor phenotype in the SMNDelta7 mouse model of spinal muscular atrophy. *Neurobiol. Dis.*, **27**, 207-219.
81 Monani, U.R., Pastore, M.T., Gavrilina, T.O., Jablonka, S., Le, T.T., Andreassi, C., DiCocco, J.M., Lorson, C., Androphy, E.J., Sendtner, M. *et al.* (2003) A transgene carrying an A2G missense mutation in the SMN gene modulates phenotypic severity in mice with severe (type I) spinal muscular atrophy. *J. Cell Biol.*, **160**, 41-52.

82 Heier, C.R., Gogliotti, R.G. and DiDonato, C.J. (2007) SMN transcript stability: could modulation of messenger RNA degradation provide a novel therapy for spinal muscular atrophy? *J. Child Neurol.*, **22**, 1013-1018.

Authorship

PNP, AHMB, and CM designed and executed experiments. SW and BK provided conceptual experimental design. VM performed animal perfusion, immunohistochemistry, and manuscript revision. AB, KF performed immunohistochemistry for stereotactic coordinate confirmation. PNP and AHMB wrote the manuscript.

Figure Legends

Figure 1. Illustration of *SMN2* exon and intron 7 with highlighted ISS-N1 and the target site for morpholino HSMNEx7D(-10-29) (MO).

Figure 2. Analysis of exon 7 incorporation in *SMN2* transcript. *Smn +/-; SMN2 +/+;* Δ7SMN +/+ mice were injected by P0 ICV with low (27цg), middle (54ug), or high dose (81цg) MO. RNA from brain (A) and spinal cord (B) tissue was isolated and cDNA amplified with SMN2 specific primers. All dosings show increased full-length *SMN2* (top band) versus exon 7 deficient *SMN2* (bottom band) at all time points (P7, P21, P45, P65) relative to scramble morpholino control (scMO) injected animals (HiC=16 copies SMN2 (8*SMN2*+/+; *Smn-/-*); WT=Wild Type). (C) Digital droplet PCR for relative full-length SMN2 (FL-*SMN2*) relative to cyclophilin; low, middle, high dose MO (dose response curve); P7 brain and spinal cord tissue. (D) Quantitative RT-PCR for full-length SMN2 in spinal cord P7-P65 (low, middle, high dose). There is increased P7 full-length SMN2, with decay at later time points.

Figure 3. Central vs. peripheral SMN2 splice modulation. (A) *RT*-PCR systemic analysis of full-length SMN2 after P0 MO ICV injection. There is no increased SMN2 exon 7 incorporation in visceral structures (heart, liver, kidney) as compared to spinal cord (n=2). (B) Digital droplet PCR (Full-Length *SMN2* relative to cyclophilin) of brain, spinal cord, heart, and liver after P0 MO ICV (54 μg) or P0 facial vein (50 μg/g) injection in *Smn +/-; SMN2 +/+;* Δ7SMN +/+ mice. Results per organ are relative to Scramble injected control, which has been set at 1 on the y-axis. There is increased CNS splice modulation after both ICV and peripheral dosing. There is no increased splicing in the heart and liver after ICV injection, suggesting limited translocation across the CSF-blood barrier or rapid systemic degradation. (C) Digital droplet PCR (FL-*SMN2* relative to cyclophilin) of brain, spinal cord, heart and liver after P0 MO ICV (54 μg) injection in *Smn -/-; SMN2 +/+;*

Δ7SMN +/+ mice; SMA scramble injected control per each organ. Results are displayed as absolute relative ratios on the y-axis. There are large increases in CNS splice modulation, and a more modest increase in liver full-length *SMN2*.

Figure 4. Analysis of SMN induction after MO delivery. *Smn +/-; SMN2 +/+;* Δ7SMN +/+ mice were injected by P0 ICV with low (27цg), middle (54ug), or high dose (81цg) MO. Quantification of SMN by human specific antibody relative to actin in brain (A) and spinal cord (B) for each dose at P7, P21, P45 and P65. All doses increased P7 SMN (strongest increase with high dose) and decay through P65 (n=3 for each dose per time point). (C-D) Representative Western blots for human SMN and actin in brain (A) and spinal cord (B) after low dose injection.

Figure 5. Motor neuron SMN expression increases in MO injected Δ7SMN SMA mice. (A-C) 54ug MO (middle) dose was injected by P0 ICV. Lumbar spinal cord tissue was harvested at P7, sectioned and stained with human specific anti-SMN KH antibody. (A) Motor neurons in the ventral horn were identified by HB9:GFP transgenic expression. (B) SMN is found in the cytoplasm and in gems in the nucleus of motor neurons, as well as other cell types, throughout the spinal cord. Insert highlights the motor neuron indicated by the arrowhead. (C) Merged image of SMN expression (red) in the motor neuron (green). Insert highlights the motor neuron indicated by the arrowhead. (D,E,F) SMN expression in a non-injected carrier control animal. (D) Motor neurons identified by HB9:GFP expression. (B) A low level of SMN expression from *SMN2* is present throughout the spinal cord. (C) Merged image of SMN expression (red) in the motor neuron (green). Scale bar = 200 μm.

Figure 6. Survival and weight gain are increased in MO treated Δ7SMN SMA animals. (A) Kaplan-Meier survival curve for low (n=8), middle (n=10), and high dose (n=13). Median survival for low (83+/-37.7 days, max 161), middle (104+/-15.0 days, max 148) and high dose (112+/-6.6 days, max 153) were not statistically different (Log Rank p>0.8 for all pairwise comparisons). Median survival for each group was significantly extended when compared with scMO (6mM, 81μg) injected Δ7SMN SMA animals (15+/-1.1 days, Log Rank p<0.001 for all pairwise comparisons). (B) MO treated Δ7SMN SMA mice increased mass nearly parallel to that of control animals (*Smn* +/+; *SMN2* +/+; SMNΔ7 +/+, scMO injection) through ~P30, at which point the mass curves leveled while control animals continued to gain weight. P80 mean: Low dose=16+/-0.9g, Middle dose: 17+/-0.6g, High dose: 19+/-1.9g, Control=22+/-1.4g. (C) Kaplan-Meier survival curve after 5 μg (n=4) and 10 μg (n=3) MO ICV P0 injection (censored, through P30).

Figure 7: Treated SMA animals have an improved motor phenotype. (A) Righting response quickly approaches 100% by P3 in ICV MO treated animals, while scMO injected SMNΔ7 SMA animals have a rapid decline in righting ability during the first week of life. No SMA animals injected with scMO were able to right after P6. (B) Mass corrected forelimb and hindlimb grip strength is equivalent between control animals (*Smn* +/+; *SMN2* +/+; SMNΔ7 +/+, scMO injection) and MO treated SMNΔ7 SMA animals (grip strength assessed at P30 in Newtons/mg body mass; Forelimb: Control 34.5+/-2.2 vs. SMA 34.2+/-2.1, Hindlimb: Control 28.2+-5.0 vs. SMA 25.8+/-4.4).

Figure 8. Alternative MO injection strategies do not increase survival beyond P0 ICV MO injection. Three cohorts of mice each received an injection of MO by P0 facial vein (50 μg/g body mass, n=3), P0 facial vein and ICV (50 μg/g peripheral, 54 μg ICV, n=5), or P0 and P30 ICV (with stereotactic guidance, 54 μg/g P0, 18 μg/g P30, n=4). Survival for all groups was equivalent to high dose P0 ICV MO injection (Log Rank p>0.09)

Figure 9. Delayed ICV injection yields intermediate weight gain and survival. (A) SMNΔ7 SMA mice treated at P4 with 54μg MO per gram body mass ('high dose' equivalent) had increased weight gain compared to SMNΔ7 SMA controls, but was less than the weight gain displayed by P0 MO treated SMNΔ7 SMA animals (P30 Mean 10.6+/-1.5g (P4) vs. 13.6+/-1.0g (P0)). (B) P4 ICV MO injected animal survival was also increased (median 41+/-14.2 days, maximum 78 days) compared to scMO injected animals (15+/-1.1 days; Log Rank $p<0.001$), but was decreased compared to SMNΔ7 SMA animals treated at P0 with high-dose MO (112+/-6.6 days, maximum 153 days, Log Rank $p<0.01$). (C) SMNΔ7 SMA mice were injected with P4 MO by facial vein. Survival was modestly extended compared to scMO injected animals, and there was a decreased survival compared to animals injected by P4 ICV MO (median 21+/-.354 days, Log Rank $p<0.014$).

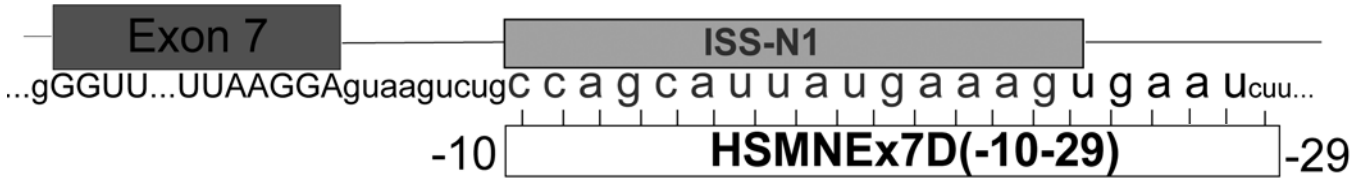
Exon 7
ISS-N1
...gGGUU...UUAAGGAguaagucugc c a g c a u u a u g a a a g u g a a ucuu...
-10
HSMNEx7D(-10-29)
-29

Fig. 1

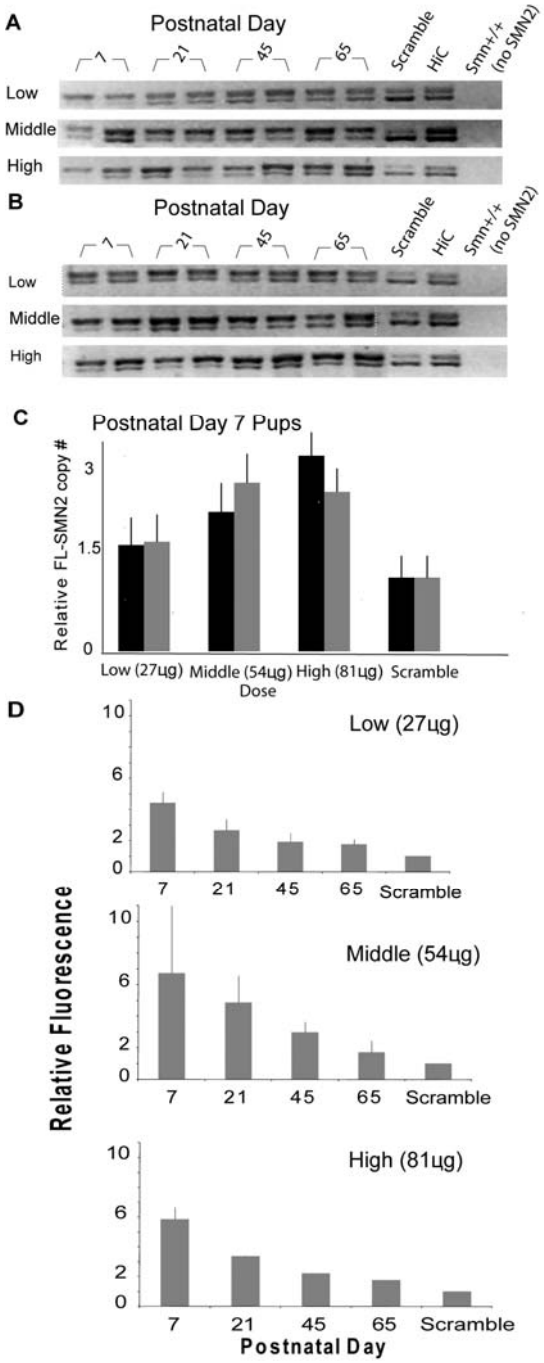
A
Postnatal Day
7
21
45
65
Scramble
HiC
Smn+/+ (no SMN2)
Low
Middle
High
B
Postnatal Day
7
21
45
65
Scramble
HiC
Smn+/+ (no SMN2)
Low
Middle
High
C
Postnatal Day 7 Pups
Relative FL-SMN2 copy #
3
1.5
0
Low (27µg)
Middle (54µg)
High (81µg)
Scramble
Dose
D
Relative Fluorescence
Low (27µg)
Middle (54µg)
High (81µg)
10
6
2
0
7
21
45
65
Scramble
Postnatal Day

Fig. 2

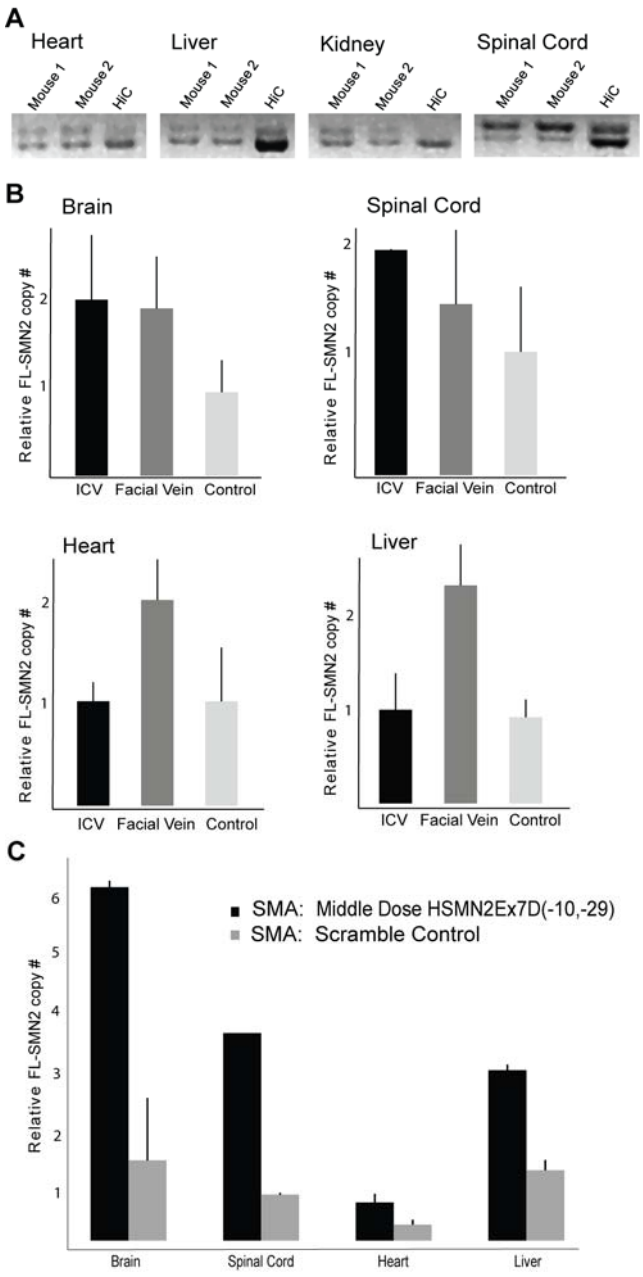
A
Heart
Liver
Kidney
Spinal Cord
Mouse 1
Mouse 2
HIC
B
Brain
Spinal Cord
Heart
Liver
Relative FL-SMN2 copy #
ICV
Facial Vein
Control
C
SMA: Middle Dose HSMN2Ex7D(-10,-29)
SMA: Scramble Control
Relative FL-SMN2 copy #
Brain
Spinal Cord
Heart
Liver

Fig. 3

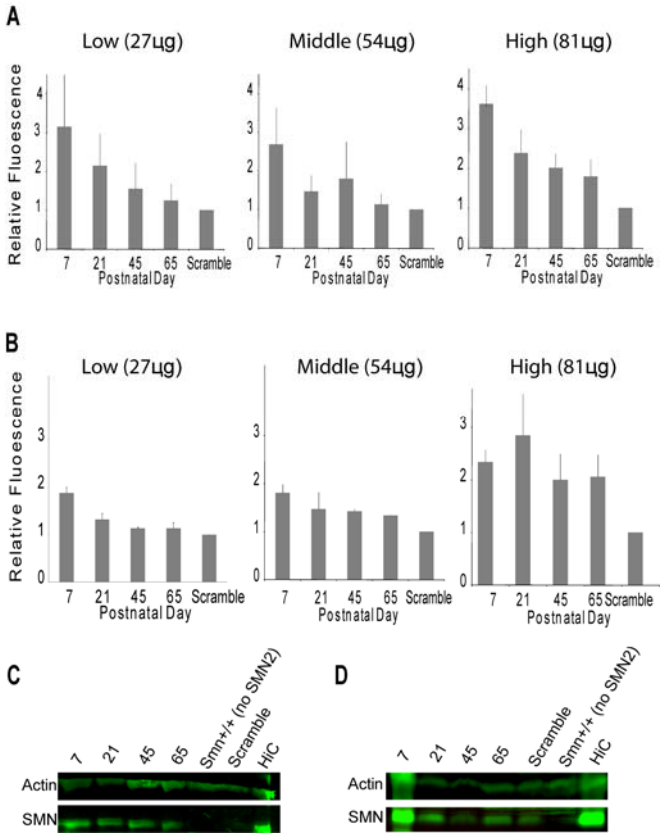
A
Low (27μg)
Middle (54μg)
High (81μg)
Relative Fluoescence
Postnatal Day
7
21
45
65
Scramble
B
C
D
Smn+/+ (no SMN2)
HiC
Actin
SMN

Fig. 4

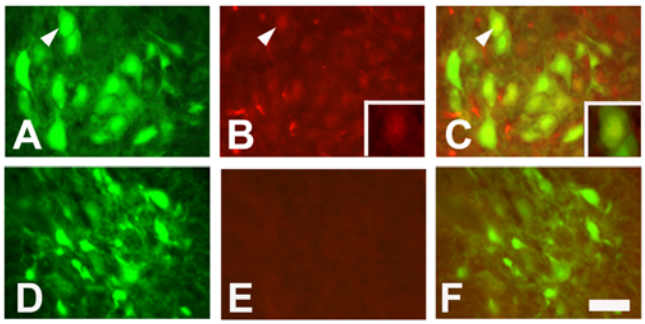

Fig. 5

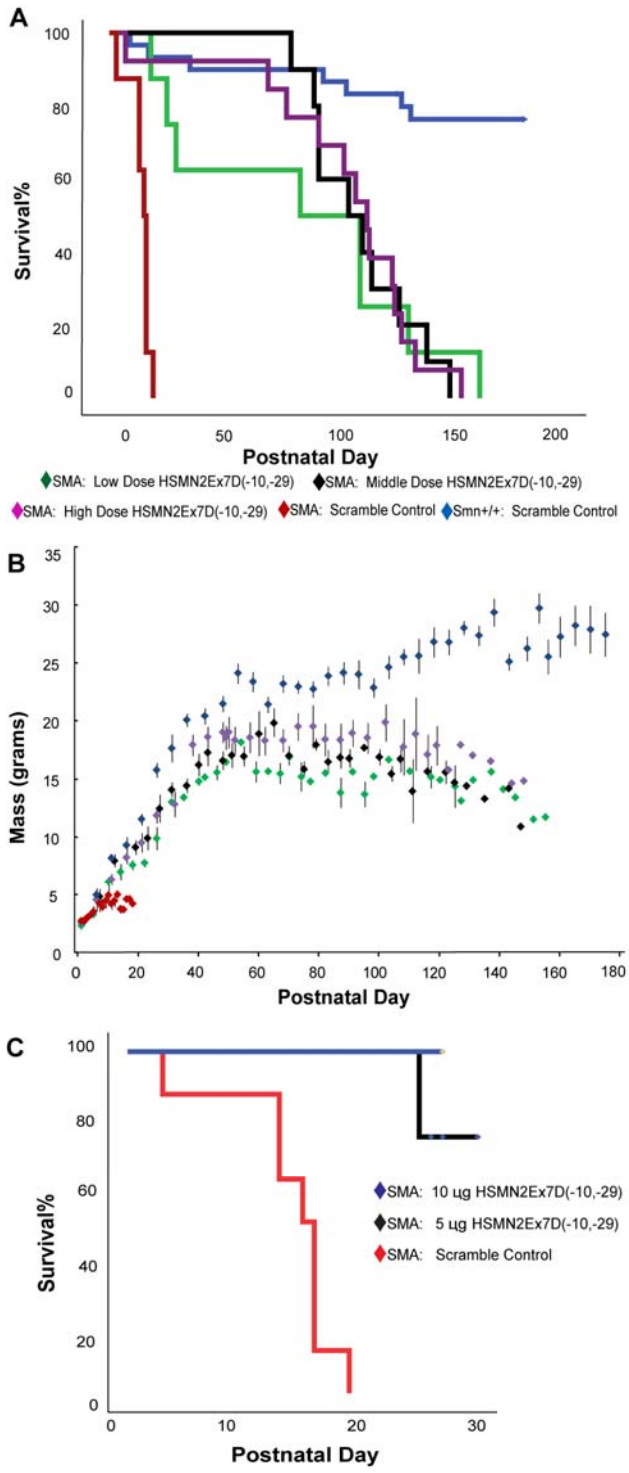
A
Survival%
Postnatal Day
SMA: Low Dose HSMN2Ex7D(-10,-29)
SMA: Middle Dose HSMN2Ex7D(-10,-29)
SMA: High Dose HSMN2Ex7D(-10,-29)
SMA: Scramble Control
Smn+/+: Scramble Control
B
Mass (grams)
Postnatal Day
C
Survival%
SMA: 10 ug HSMN2Ex7D(-10,-29)
SMA: 5 ug HSMN2Ex7D(-10,-29)
SMA: Scramble Control
Postnatal Day

Fig. 6

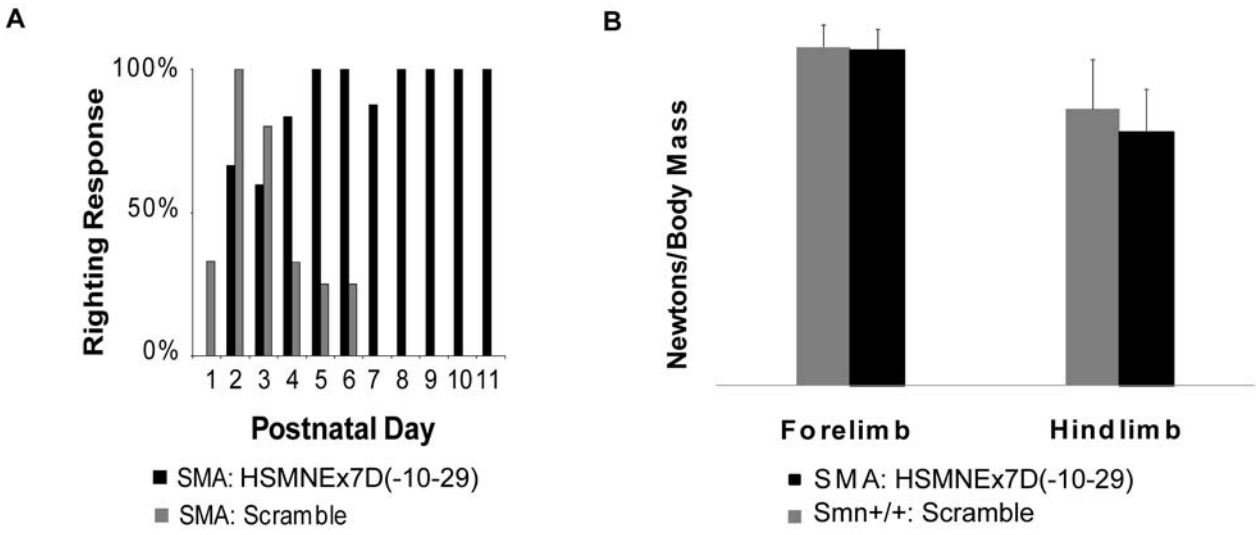
A
100%
50%
0%
Righting Response
1 2 3 4 5 6 7 8 9 10 11
Postnatal Day
SMA: HSMNEx7D(-10-29)
SMA: Scramble
B
Newtons/Body Mass
Forelimb
Hindlimb
SMA: HSMNEx7D(-10-29)
Smn+/+: Scramble

Fig. 7

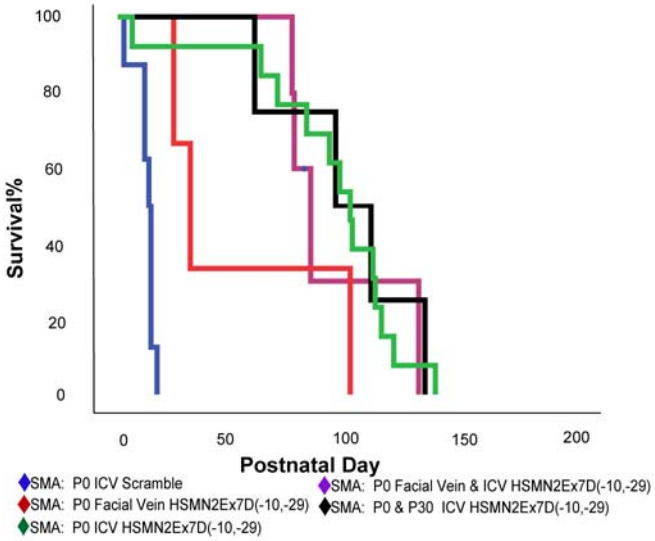
100
80
60
40
20
0
Survival%
0
50
100
150
200
Postnatal Day
SMA: P0 ICV Scramble
SMA: P0 Facial Vein HSMN2Ex7D(-10,-29)
SMA: P0 ICV HSMN2Ex7D(-10,-29)
SMA: P0 Facial Vein & ICV HSMN2Ex7D(-10,-29)
SMA: P0 & P30 ICV HSMN2Ex7D(-10,-29)

Fig. 8

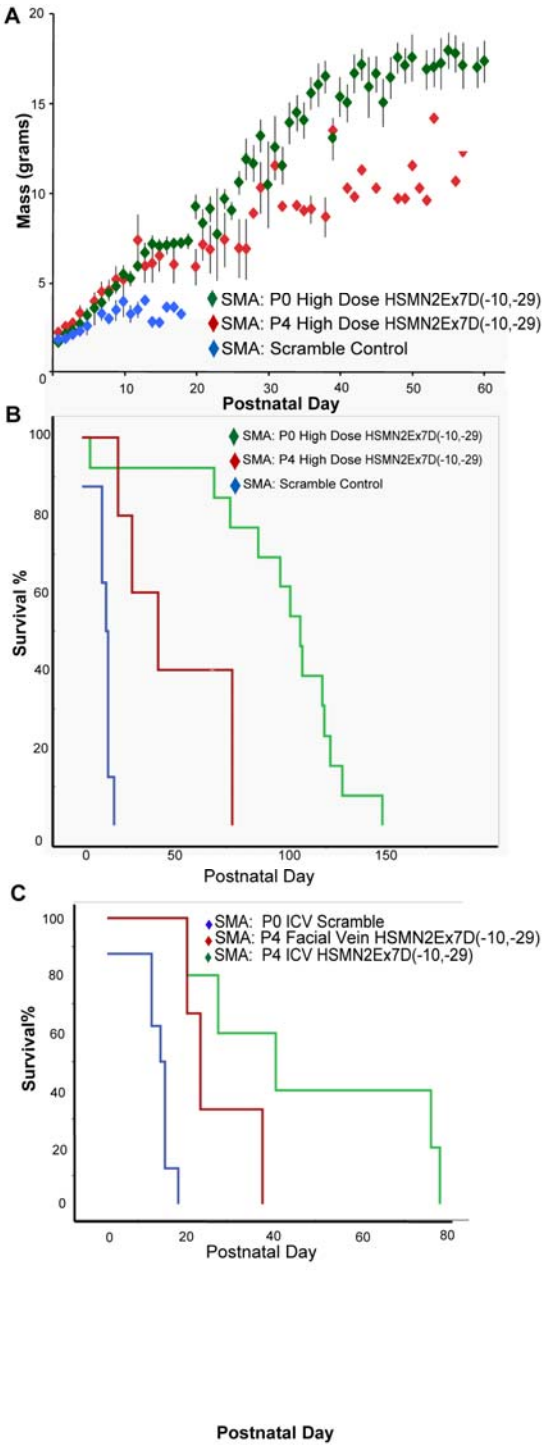
A
Mass (grams)
Postnatal Day
SMA: P0 High Dose HSMN2Ex7D(-10,-29)
SMA: P4 High Dose HSMN2Ex7D(-10,-29)
SMA: Scramble Control
B
Survival %
Postnatal Day
SMA: P0 High Dose HSMN2Ex7D(-10,-29)
SMA: P4 High Dose HSMN2Ex7D(-10,-29)
SMA: Scramble Control
C
Survival%
Postnatal Day
SMA: P0 ICV Scramble
SMA: P4 Facial Vein HSMN2Ex7D(-10,-29)
SMA: P4 ICV HSMN2Ex7D(-10,-29)
Postnatal Day

Fig. 9